

# Thermotropic Polyesters with Flexible Spacers Bearing Ether Bonds in Asymmetric Position

Pablo Bello, Antonio Bello,\* Evaristo Riande, and Nicholas J. Heaton

Instituto de Ciencia y Tecnología de Polímeros (CSIC), Juan de la Cierva 3, 28006 Madrid, Spain

Received July 14, 2000; Revised Manuscript Received September 29, 2000

**ABSTRACT:** The synthesis of several polyesters from *p,p'*-bibenzoic acid and diols bearing ether bonds in asymmetric positions is described. The polyesters develop smectic mesophases, the type of which depends on the chemical structure of the spacer. The ether groups and the asymmetry of the spacers stabilize the liquid crystalline order in these polymers. Glass transition and isotropization temperatures, enthalpies, and entropies of the thermotropic polyesters are reported. Comparison of the melting entropies with the conformational entropies of the chains suggests a great disorder in the mesophases of thermotropic polyesters. For some polyesters, the stretched polymer chains do not follow the direction of the fiber axis, an unusual phenomenon that has already been described for some polybibenzoates with aliphatic separators. The influence of the strain rate on the anomalous flow is discussed.

## Introduction

Several papers have been published showing the ability of polyesters derived from bibenzoic acid to form thermotropic liquid crystals.<sup>1–5</sup> The mesogenic units separated by flexible spacers develop smectic mesophases whose nature depends on the structure and the even–odd character of the spacers. Polybibenzoates with all methylenic groups in the linear flexible backbone form unstable mesophases that eventually evolve to three-dimensional crystalline structures. Bidimensional → tridimensional order transitions in these thermotropic polyesters are usually fast, and the thermodynamic behavior is monotropic. Both the smectic mesophase–crystal transformation rate and the thermal properties depend on the stiffness of the molecular chains. The stiffness is governed by the number of conformations permitted to the chains, which can be modified by inserting bulky side groups and/or ether groups along the paraffinic spacer.

The information at hand suggests<sup>6</sup> that, as a result of substituting methylenic groups by a ether linkages in the paraffinic spacer, the thermal transitions of thermotropic polyesters are shifted to lower temperatures. Moreover, bidimensional → tridimensional order transitions are totally or partially inhibited, the mesophases are considerably stabilized, and the thermodynamic behavior becomes enantiotropic.

Since the steric requirements for the formation of mesophases are less restrictive than for the development of three-dimensional order, copolymerization usually favors mesophase structures. Therefore, the use of diols bearing ether bonds in asymmetric positions gives rise to random copolymeric structures along the polyester backbone that favor the stabilization of the mesophases. The purpose of this work is to consider how the asymmetric nature of the spacer affects the development of mesophases in thermotropic polyesters. With this aim, a series of four diols possessing ether linkages asymmetrically positioned were synthesized by addition of propylene glycol, ethylene glycol, diethylene glycol, and 2-methyltrimethylene glycol to the cyclic trimethylene oxide. The chemical structures of these ether–diols are shown in Figure 1.

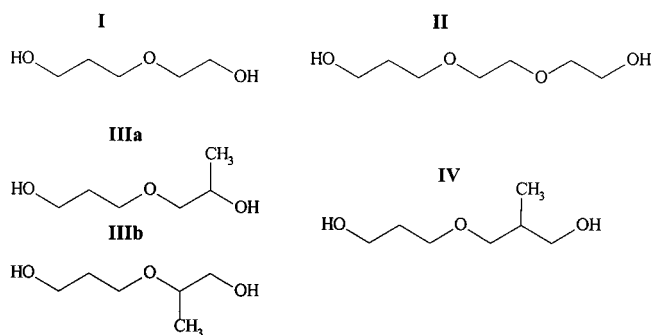


**Figure 1.** Oxyethylenes synthesized by oxetane with ethylene glycol (I), diethylene glycol (II), 1,2-propanediol (IIIa and IIIb, 65–35%), and 2-methyl-1,3-propanediol (IV).

In this work, the polycondensation of bibenzoic acid and the ether–diols is reported, emphasizing both the characteristics of the mesophases and the phase transitions of the resulting polyesters. Three of these polyesters show anomalous orientation when they are stretched at room temperature, similar to that reported for a few other thermotropic polymers subjected to either shearing<sup>7,8</sup> or drawing from the melt.<sup>9–11</sup> Special attention is devoted to the influence of the drawing rate on the relative orientations of the fiber and the smectic layers of the polyester PTMTB whose structure is shown in Figure 3. Finally, the conformational entropy of the polyesters is calculated and compared with the entropy involved in the mesophase → isotropic melt transition.

## Experimental Part

**Materials.** Ethylene glycol, diethylene glycol, 1,2-propanediol, and 2-methylpropanediol were distilled prior to their use. 4,4'-Biphenildicarboxylic acid (Aldrich) was crystallized from ethanol. Oxetane (Aldrich) was also purified by distillation from several sodium mirrors in a vacuum line.

**Ether–Diols Synthesis.** The ether–diols used as flexible spacers were prepared under nitrogen atmosphere or vacuum, by adding oxetane to an excess of the corresponding diol, using sulfuric acid as catalyst. In a typical reaction, 0.1 mol of sulfuric acid was slowly dissolved in approximately 1.5 mol of the glycol of interest contained in a round-bottom flask cooled with water. To this solution was added 0.15 mol of purified

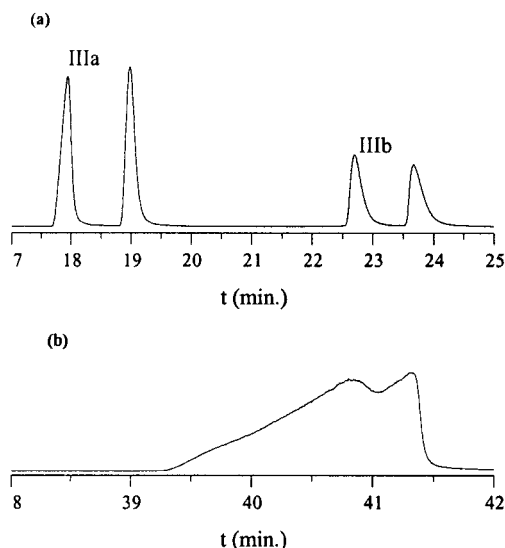


**Figure 2.** Gas chromatography of the products of the reaction of oxetane (a) with 1,2-propanediol and (b) with 2-methyltrimethylene glycol.

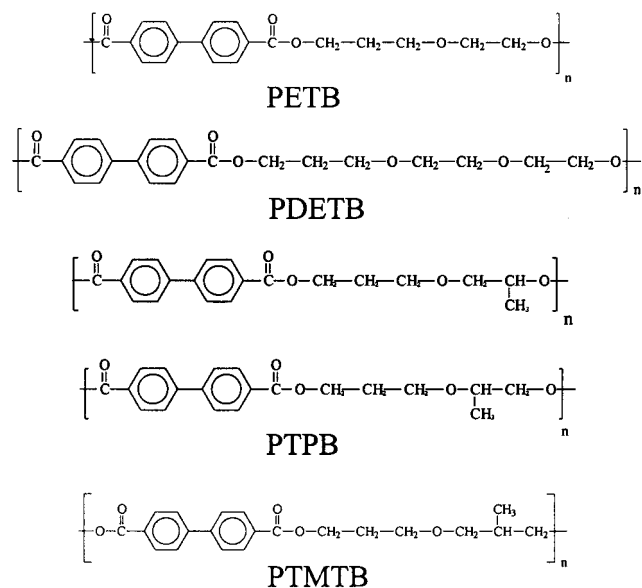


**Figure 3.** Molecular structures of the polybibenzoates investigated.

oxetane dropwise for nearly 2 h. The reactions were terminated with sodium bicarbonate, filtered, washed with water, extracted with chloroform, and distilled several times under vacuum. In all cases, the ether-glycol yield was higher than 75%. Small amounts of trimers, detected in the reaction products by gas chromatography, were easily separated by distillation in a vacuum. Gas chromatography was also used to identify the ether glycol isomers formed, the corresponding chromatograms being shown in Figure 3. The products were characterized by <sup>1</sup>H and <sup>13</sup>C NMR in deuterated chloroform, using a Varian 300 MHz spectrometer.

**Polyesters Synthesis.** The synthesis of diethyl *p,p'*-bibenzoate was performed in two steps. In the first step, 0.6 mol of thionyl chloride was added dropwise, under ice cooling, to 0.1 mol of *p,p'*-biphenol. Then pyridine was added as catalyst, and the reaction mixture was stirred at 60 °C for 10 h. The *p,p'*-biphenyl dichloride formed was separated by filtration and washed with dry benzene. In the second step, diethyl *p,p'*-bibenzoate was rapidly obtained by addition at room temperature of an EtNa/EtOH solution to *p,p'*-biphenyl dichloride. The solvent was eliminated at reduced pressure, and the diethyl *p,p'*-bibenzoate obtained was dissolved in chloroform and washed with water. The ester was separated in the organic

**Table 1.** Intrinsic Viscosity, Number- and Weight-Average Molecular Weights, and the Molecular Weight at the Peak

polymer	$[\eta]$ , dL/g	$10^{-3} M_n$	$10^{-3} M_w \times M_w$	$10^{-3} M_p \times M_p$
PETB	0.52	10	27	23
PDETb	0.30	10	24	22
PTPB	0.35	12	33	26
PTMTB	0.54	14	24	32

layer, which was further dried over MgSO<sub>4</sub>. Chloroform was eliminated at reduced pressure and the ester recrystallized from ethanol. Yield 67%.

The four polyesters used in this study were obtained by melt transesterification reaction of diethyl *p,p'*-bibenzoate and the corresponding ether diol, using tetraisopropyl titanate (TIPT) as catalyst. The usual run procedure was as follows: First, a mixture of diethyl *p,p'*-bibenzoate (0.1 mol) and glycol (0.12 mol) was heated at 190–200 °C under stirring. Then 0.03 mL of TIPT was added to the mixture which was stirred under a nitrogen atmosphere for several hours. Finally, polycondensation was carried out at higher temperature (200–250 °C) under reduced pressure (0.01 mmHg) for 2 h. The polymers were dissolved in chloroform and precipitated with methanol. The recovered materials were close to 90% of the theoretical yield. Schemes of the structural units are shown in Figure 2.

The polyesters were characterized by GPC, using a Waters 150C apparatus. The chromatograms were obtained at 30 °C in chloroform, using a set of PL gel columns (2 mixed bed of 5  $\mu$ m). A dual detector, differential refractometer, and viscometer (Viscotek 150 R) working at 30 °C were connected to the columns. The flow rate was 1.0 mL/min, the sample concentration 5 mg/mL, and the volume of injection 100  $\mu$ m. Twelve samples of monodisperse polystyrene were used as standards, considering the  $M_{peak}$  representative of the whole sample. The universal calibration method was used to characterize the molecular weights of the polyesters. The results comprising intrinsic viscosities, number- and weight-average molecular weights, and the molecular weight at the peak,  $M_{peak}$ , are given in Table 1.

**Calorimetric and X-ray Measurements.** Differential scanning calorimetry (DSC) was performed with a Perkin-Elmer DSC-7 calorimeter. The temperature and the heat flow were calibrated at different cooling rates using standard materials.

Fibers were obtained by stretching a piece of each thermotropic polyester at room temperature or just above  $T_g$ . The drawing (or stretching) ratios were always close to 1:6. Fiber WAXD patterns were obtained at room temperature using a flat-plate camera attached to a Philips 2 kW tube X-ray generator.

## Results and Discussion

In the case of the reaction of oxetane and racemic 1,2-propanediol (diol III, Figure 1), the different reactivities of the two alcoholic groups, together with the racemic nature of the diol III, give rise to the formation of four products whose presence in the reaction medium was confirmed by gas chromatography (see Figure 2). The crude product was analyzed by gas chromatography using a column filled with hypermethylated  $\beta$ -cyclodextrin, with programmed temperature from 80 to 190 °C. Four chromatographic peaks were observed, corresponding to the *R,S*-isomers of the two possible ether glycols that can be formed. No further separations of these enantiomers were necessary to obtain grams of the products. Owing to the differences in reactivity of the secondary versus primary alcohols in the propylene glycol, the proportions of the two possible ether glycols in the sample are not equivalent. About 65% of the product corresponds to the ether glycol in which one end is a primary alcohol and the other a secondary alcohol,

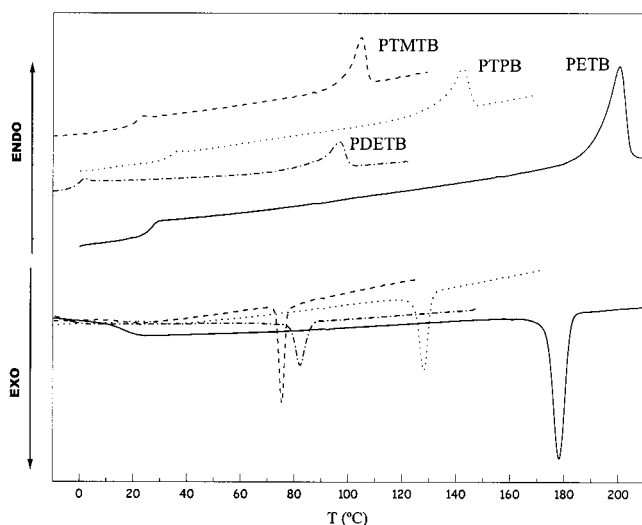


**Figure 4.** Heating and cooling DSC curves (rate 10 °C min<sup>-1</sup>) corresponding to PETB, PDETb, PTPB, and PTMTB samples.

**Table 2.** Glass Transition Temperatures,  $T_g$ , Isotropization Temperatures,  $T_i$ , Isotropic  $\rightarrow$  Smectic Transition,  $T_c$ , Isotropization Enthalpies,  $\Delta H_i$ , and Isotropization Entropies,  $\Delta S_i$ , of the Liquid Crystals, Conformational Entropies,  $\Delta S_c$ , Type of Mesophases, and Thickness of the Smectic Layers,  $d_{exp}$

	PETB	PDETb	PTPB	PTMTB
$T_g$ , °C	25.0	-1.7	32.9	20
$T_i$ , °C	199.2	96.7	142.7	105.1
$T_c$ , °C	178.3	82.1	128.3	75.3
$\Delta H_i$ , kcal mol <sup>-1</sup>	1.38	0.85	1.17	1.02
$\Delta S_i$ , cal mol <sup>-1</sup> K <sup>-1</sup>	2.92	2.30	2.8	2.70
$\Delta S_c$ , cal mol <sup>-1</sup> K <sup>-1</sup>	16.1	20.9	15.0	18.5
mesophase	S <sub>C</sub>	S <sub>CA</sub>	S <sub>A</sub>	S <sub>CA</sub>
$d_{exp}$ , Å	16.8	18.9	19.5	16.6

whereas 35% of the product is made up of ether glycol molecules with only primary alcohols at both ends. The proportion of *R,S*-isomers in both compounds is 50%. In the case of the addition of 2-methyl-1,3-propanediol to oxetane (diol IV), again two chromatographic peaks of the same intensity were obtained corresponding to the two *R,S*-isomers, confirming the effectiveness of hypermethylated  $\beta$ -cyclodextrin as stationary phase for the separation of enantiomers from a racemic mixture.

Figure 4 shows a set of DSC heating and cooling curves for the polyesters synthesized in this work; in all the cases rates of 10 °C/min for heating and cooling were used. The pertinent results and thermodynamic data are collected in Table 2. All the heating and cooling DSC scans exhibit similar features with some variations in the location of their thermal transitions and thermodynamic parameters. Starting from the melt, the cooling thermograms show first an exothermic peak corresponding to the formation of a mesophase, whereas at lower temperatures a change in the specific heat associated with the glass transition appears. On heating, both the glass transition and the endothermic peak arising from the smectic–isotropic transition are observed. Thus, the transition is enantiotropic for all these polymers. More ordered structures are not apparently developed by three of the polyesters, PDETb, PTPB, PTMTB, held at room temperature for long time. However, the DSC thermograms of PETB, annealed at room temperature for several months, exhibit two small peaks located in the vicinities of 60 and 110 °C,

respectively. These peaks are associated with more ordered mesophases, as proved by the appearance of a splitting of the external halo in the X-ray diffraction pattern.

The only structural change observed in the samples having the glass transition temperature close to room temperature, after annealing them at temperatures near  $T_g$ , is related to their densification or hardening. This fact was earlier interpreted as a physical aging effect.<sup>12</sup> These results clearly show the stabilizing effect of the spacers containing ether groups on the structure of the mesophases.

The X-ray diffraction patterns of the polyesters quenched at room temperature from the melt show their smectic character. All of them present a sharp inner reflection, attributed to the smectic layers. A second order is also visible, and an outer broad halo that shows the liquidlike packing of the molecules. The Bragg spacing of the inner reflections are given in Table 2. The type of smectic mesophase could be deduced from the oriented diffraction patterns. For example, the X-ray pattern of the oriented PETB sample, manually stretched at room temperature, exhibits a broad outer reflection with maximum intensity centered on the equator, whereas the inner reflection is divided into four spots, out of meridional, one in each quadrant. This pattern, shown in Figure 5, corresponds to a S<sub>C</sub> structure. The tilt angle between the molecular chain axis and the layer normal, directly measured on the photo, is about 28° at room temperature.

The X-ray diffraction for the oriented PDETb sample manually stretched in the same conditions as before displays an anomalous behavior. The sharp inner reflection appears like a spot on equatorial, and the broad outer reflection splits into two portions on both sides of the meridional, indicating that the mesophase is of the type S<sub>CA</sub>. Here the tilt direction of the axis of the mesogenic groups alternates between neighboring layers. The orientation geometry is unusual in that the smectic layers orient parallel to the stretching direction.

A similar behavior was observed in the X-ray diffraction of PTPB manually stretched without controlling the strain rate. By comparing the diffraction pattern of the thermotropic polyester with that of the isotropic sample, one can see that the sharp inner reflection is transformed in two spots; also, a second order on the equatorial is seen. For the outer halo the maximum intensity is concentrated on the meridional, following the fiber direction. This sample has the characteristics of a S<sub>A</sub> mesophase, since the normal to the layer and the axis of the repeating unit of the macromolecule coincide. Once again, the diffraction pattern shows that the smectic planes are perpendicular to the fiber axis. Apparently, not all the material is involved in this particular orientation. A careful inspection of the diffraction pattern reveals a mixture of two materials: a well-oriented material, as the well-defined layer spots suggest, and a poorly oriented material reflected by the continuous rings superimposed over the layer spots.

Preliminary tests showed the sensitivity of the direction of orientation of PTMTB to the strain rate. For this reason these samples were stretched to a 1:6 ratio in an Instron machine, at three different drawing rates: 0.5, 10, and 500 mm/min. The stress–strain curves are similar to those displayed by many semicrystalline and glassy polymers. At short elongations, the stress is proportional to the strain, and therefore the material

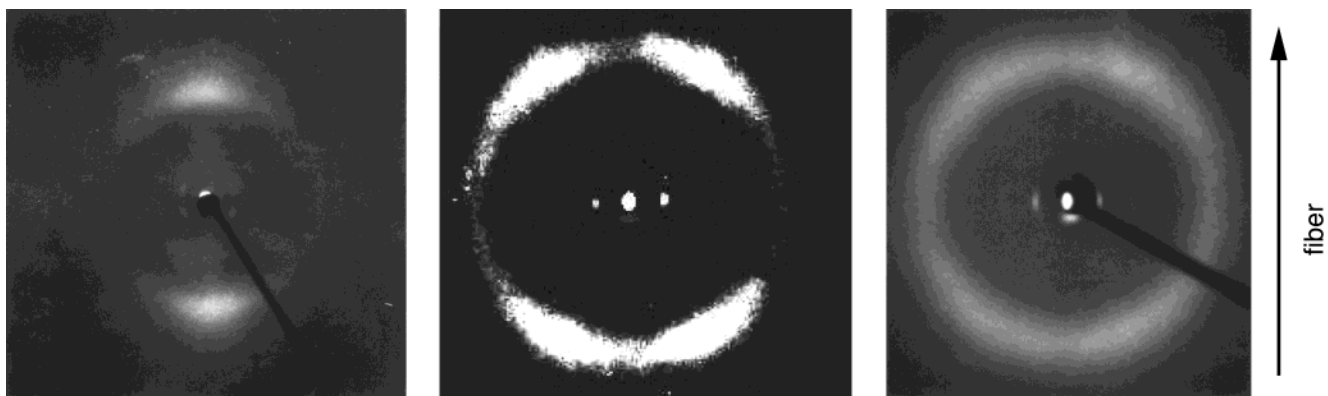


**Figure 5.** X-ray diffraction for fibers of (left) PETB, (middle) PDETb, and (right) PTPB drawn at room temperature. The fiber axis is in the vertical direction.

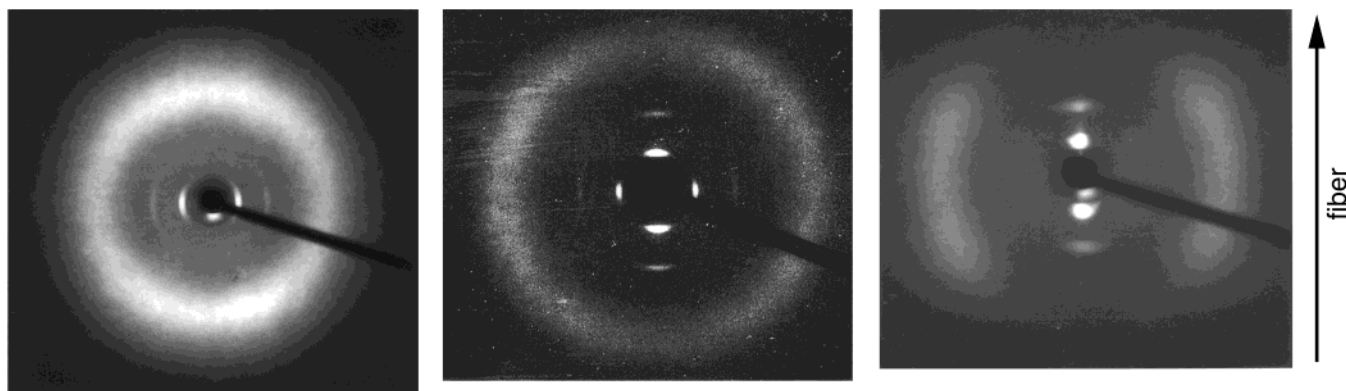


**Figure 6.** X-ray photographs for a fiber of PTMTB, drawn at 40 °C at 0.5 mm/min (left), 10 mm/min (center), and 500 mm/min (right). The fiber axis in the vertical direction.

shows elastic behavior. After a characteristic value of the tensile stress is reached, called the yield stress, the material flows and the stress remains nearly constant until its rupture. It is noteworthy that although the stress-strain curves are vertically shifted to higher stresses with increasing drawing rates, the yield stress appears at approximately the same elongation ratio.

As can be seen in Figure 6, the fiber stretched to the higher drawing rate presents the usual diffraction expected for polybibenzoates with an odd number of groups in the spacer, in which the axes of the mesogens and of the spacer do not coincide. The outer diffraction splits into two, above and below the equator, with a minimum of intensity in this axis. The diffraction due to the smectic layers appears like spots in the meridional, a feature that corresponds to a mesophase<sup>3,13,14</sup> of type  $S_{CA}$ . The fiber oriented at the lower drawing rate presents a similar diffraction pattern, though its orientation is rotated 90° (Figure 6). This implies that the normal to the smectic layers is perpendicular to the direction of the fiber. The diffraction pattern of the fiber stretched at the intermediate drawing rate of 10 mm/min, shown in Figure 6, indicates the coexistence of the orientations corresponding to fibers stretched at 0.5 and 500 mm/min. The pattern looks as if the fibers had been simultaneously stretched in two perpendicular directions. This kind of dual orientation can only be obtained in the fibers of PTMTB by stretching them at intermediate drawing rates. A close inspection of this diffraction pattern suggests that there is good orientation in directions parallel and perpendicular to the fiber. No residual rings of unoriented polymer are observed. The parallel and perpendicular spots are of roughly the same intensity, and both exhibit second order.

The fact that on stretching the chains do not follow the direction of the stress is difficult to reconcile with the macromolecular character of thermotropic polyesters. Stretching in this situation may occur as if the smectic layers slipped relative to each other so as to lie parallel to the fiber axis.<sup>11</sup> This type of flow is possible in low molecular weight smectic layers but is not acceptable in polymers since the mesogenic groups in neighboring chains are linked by the flexible spacer. To explain the orientation of the smectic layers whose normal is perpendicular to the fiber direction, Watanabe et al.<sup>15</sup> postulated the existence of domains in the smectic field so that the flow would occur along the domains boundaries. Irregular chain folding in the domains that would make possible the slippage that would arise from the interplay between long-range orientational order of the liquid crystal and the polymeric tendency to maximize entropy. De Gennes<sup>16</sup> pointed out that semiflexible long chains in the nematic phase might recover some part of the configurational entropy lost due to the ordering of the mesogenic units by forming hairpin foldings. Therefore, the dependence of the orientation on the strain rate could be explained by assuming the existence of domains (type A) in which the smectic layer normals are poorly ordered with respect to the fiber axis. These domains could coexist with others (type B) in which the normal to the smectic layers are poorly ordered with respect to axes orthogonal to the fiber direction. According to this, the orientation at high strain rate would involve type A domains whereas at very low strain rate domains of type B would slip over each other.

We now analyze the disorder in the mesophases. A variety of conformations of the repeating unit having

suitable extensions and favorable angular correlations of the successive rigid cores participate in the formation of liquid crystalline order. It is therefore tempting to compare the melting entropy of the mesophases with the conformational entropy involved in the transition from a perfect tridimensional crystal to the melt. Although the conformational entropy may be the most important contribution to the melting entropy, other contributions corresponding to long-range disorder and changes in volume also intervene. The conformational entropy is related to the rotational partition function  $Z$  by the following expression<sup>17,18</sup>

$$\Delta S_c = R \left( \ln Z + T \frac{d \ln Z}{dT} \right) \quad (1)$$

where  $Z$  is given by<sup>19</sup>

$$Z = \mathbf{J}^* \left[ \prod_{i=2}^{n-1} \mathbf{U}_i \right] \mathbf{J} \quad (2)$$

In this equation each statistical weight matrix  $\mathbf{U}$  contains the statistical weights for all conformations of a successive pair of skeleton bonds, and  $\mathbf{J}^*$  and  $\mathbf{J}$  are respectively row and column vectors that extract the desired terms from the matrix product. In the formulation of the statistical weight matrices, the C(O)–O bonds of the ester were assumed to be restricted to trans states. Because coplanarity of the carbonyl group with the phenyl group guarantees maximum overlapping of electrons of the participant atoms, the skeletal bonds  $\text{C}^{\text{ar}}\text{--C}(\text{O})$  bonds are restricted to two rotational states,<sup>20</sup> 0° and 180°. The strong interactions occurring between the neighboring hydrogen atoms of the two phenyl groups of the mesogenic moiety are alleviated by rotations about the  $\text{C}^{\text{ar}}\text{--C}^{\text{ar}}$  with potential minima located at 45°, 135°, 225°, and 315°. Three rotational potential minima are assumed for the rest of skeletal bonds of the repeating unit of the polymers. Information concerning the conformational energies of the rotational states was obtained from conformational studies carried out on polyethers and polyesters.<sup>21</sup> Values of the conformational entropy for several polyesters are given in the sixth row of Table 1. It can be seen that the conformational entropy is significantly higher than the melting entropy associated with the transition liquid crystalline  $\rightarrow$  isotropic liquid, confirming greater conformational disorder of the mesogenic phase relative to that of the three-dimensional crystal. Thermodynamic arguments suggest that the entropy change due to the restriction of conformations in the smectic phase<sup>22,23</sup> is given by

$$\Delta S = -R \ln p + \Delta h/T_s \quad (3)$$

where  $p$  is the fraction of conformers in the melt allowed in the smectic phase,  $T_s$  is the transition temperature, and  $\Delta h$  is the difference between the average energy of all the conformers and the average energy of the conformers allowed in the smectic phase. In the case of PTMTB, the thickness of the smectic layers is 16.6 Å, and the values computed for  $p$  and  $\Delta h$  are 0.17 and 150 cal mol<sup>−1</sup>, respectively. Hence, the change in conformational entropy involved in the liquid crystal  $\rightarrow$  isotropic liquid transition of this polymer is ca. 3.9 cal mol<sup>−1</sup> K<sup>−1</sup>. Therefore, the confinement of the chains in the smectic

layers greatly decrease their conformational entropies. It should be pointed out that the value of  $\Delta S$  (3.9 cal mol<sup>−1</sup> K<sup>−1</sup>) is rather close to the experimental value of 2.70 cal mol<sup>−1</sup> K<sup>−1</sup> given for  $\Delta S_i$  in Table 1. In further work this method will be used to interpret in more detail the isotropization entropies involved in the transitions of the polyesters described in this study.

Finally, a few comments are in order concerning the glass transition temperature of the thermotropic polyesters studied in this work. The glass transition of polymers is related to their molecular flexibility. This may be expressed in terms of either the rotational partition function calculated by normalizing to the unit the state of higher statistical weight or the conformational entropy. The higher the rotational partition function or the conformational entropy, the lower is the glass transition. This reasoning may be qualitatively sound for amorphous nonpolar polymers but fails for liquid crystalline polymers. In this case, the conformational entropy is calculated taking into account only those conformations compatible with the smectic phases rather than the entire range of conformers.

## Conclusions

The presence of ether groups in the spacers stabilizes the mesophases in thermotropic polyesters. For three of the uniaxially oriented polyesters studied in this work, the fiber axis is parallel to the direction of the smectic layers. Within the interval of drawing rates studied, only for PTMTB the angle between the fiber axis and the direction of the smectic layers depends on the drawing rate. For high and low drawing rates the angle is 0° and 90°, respectively, whereas for intermediates values of the draw rate the two angles coexist. This behavior suggests that displacement of the mesogenic groups perpendicular to the fiber axis involves less energy than parallel to the axis. However, the structural features responsible for the differences observed in the stretching flow behavior of polymers with such similar structural characteristics are not yet clear.

## References and Notes

- (1) Watanabe, J.; Hayashi, M. *Macromolecules* **1989**, *22*, 4083.
- (2) Bello, A.; Pérez, E.; Marugán, M. M.; Pereña, J. M. *Macromolecules* **1990**, *23*, 905.
- (3) Watanabe, J.; Hayashi, M.; Nakata, Y.; Niori, T.; Tokita, M. *Prog. Polym. Sci.* **1997**, *22*, 1053.
- (4) Bello, A.; Pereña, J. M.; Pérez, E.; Benavente, R. *Macromol. Symp.* **1994**, *84*, 297.
- (5) Pérez, E.; Pereña, J. M.; Benavente, R.; Bello, A. In *Handbook of Engineering Polymeric Materials*; Cheremisinoff, N. P., Ed.; Marcel Dekker: New York, 1997; Chapter 25.
- (6) Bello, A.; Riande, E.; Pérez, E.; Marugán, M. M.; Pereña, J. M. *Macromolecules* **1993**, *26*, 1072.
- (7) Romo-Uribe, A.; Windle, A. H. *Macromolecules* **1996**, *29*, 6246.
- (8) Alt, D. J.; Hudson, S. D.; Garay, R. O.; Fujishiro, K. *Macromolecules* **1995**, *28*, 1575.
- (9) Krigbaum, W. R.; Watanabe, J. *Polymer* **1983**, *24*, 1299.
- (10) Leland, M.; Wu, Z.; Chhajaj, M.; Ho, R.; Cheng, S. Z. D.; Keller, A.; Kricheldorf, H. R. *Macromolecules* **1997**, *30*, 5249.
- (11) Tokita, M.; Osada, K.; Kawauchi, S.; Watanabe, J. *Polym. J.* **1998**, *30*, 687.
- (12) Benavente, R.; Pereña, J. M.; Bello, A.; Pérez, E. *Polym. Bull.* **1995**, *34*, 635.
- (13) Watanabe, J.; Kinohita, S. *J. Phys. II* **1992**, *2*, 1237.
- (14) Tokita, M.; Osada, K.; Watanabe, J. *Liq. Cryst.* **1998**, *24*, 477.
- (15) Tokita, M.; Osada, K.; Watanabe, J. *Liq. Cryst.* **1997**, *23*, 435.
- (16) deGennes, P. G. In *Polymer Liquid Crystals*; Ciferri, A., Krigbaum, W. R., Mayer, R. B., Eds.; Academic Press: New York, 1982; p 124.

- (17) Brant, D. A.; Miller, W. G.; Flory, P. J. *J. Mol. Biol.* **1967**, *23*, 47.
- (18) Riande, E. *Eur. Polym. J.* **1978**, *14*, 885.
- (19) Flory, P. J. *Statistical Mechanics of Chain Molecules*; Wiley-Interscience: New York, 1969.
- (20) Riande, E.; Saiz, E. *Dipole Moments and Birefringence of Polymers*; Prentice Hall: Englewood Cliffs, NJ, 1992.
- (21) Abe, A.; Mark, J. E. *J. Am. Chem. Soc.* **1976**, *98*, 6468.
- (22) González, C.; Riande, E.; Bello, A.; Pereña, J. M. *Macromolecules* **1988**, *21*, 3230.
- (23) Pérez, E.; Riande, E.; Bello, A.; Benavente, R.; Pereña, J. M. *Macromolecules* **1992**, *25*, 605.

MA001225X